THE USE OF SATELLITE RADIANCE MEASUREMENTS IN THE ECMWF ANALYSIS SYSTEM

G.A. Kelly*
European Centre for Medium Range Weather Forecasts
Reading, UK

1. INTRODUCTION

This study gives some preliminary results of new software to calculate from the ECMWF system the spacial error structure of satellite retrieved temperature profiles.

These statistics are calculated over the Central United States (U.S.) using ECMWF analyses and the results are compared with previous studies of Schlatter and Branstator (1979), Schlatter (1980). The software package is also extended to explore the use of clear column satellite radiances directly in the ECMWF analyses system. An important consideration is not the use redundant information otherwise the computational overheads in the Optimum Analyses could be very large due to the large number of radiances in each satellite observation.

2. SPACECRAFT SOUNDING SYSTEM

The TIROS-N NOAA A-G series of satellites began operating in October 1978. These satellites are high-quality observation platforms supplying large amounts of data describing the Earth's surface and enveloping atmosphere. The TIROS-N Operational Vertical Sounder (TOVS) (Smith, et al. (1979)) instrument packages on board all these satellites allow vertical temperature and moisture structures (soundings) to be calculated between the surface and the stratopause. Ideally two satellites are operational and are in sun-synchronous polar orbit at any one time. This implies a full global coverage by these satellites every six hours.

The TOVS package consists of three radiance measuring instruments: the High-resolution Infrared Radiation Sounder (HIRS), sampling at 20 infrared frerquencies, the Microwave Sounding Unit (MSU), sampling at four microwave frequencies, and the Stratospheric Sounding Unit (SSU), sampling at three additional infrared frequencies. The HIRS instrument resolves a mean area 30 km in diameter at the sub-satellite point, whereas the MSU resolves a circular area of 110 km in diameter. There are 56 fields of view (fov) within each scan line width of approximately 2,250 km for the HIRS instrument. Only 11 fovs are completed in every MSU scan line in the time the HIRS instrument takes for five scan lines or 280 fovs. For both instruments, the fov "footprints" become elliptical and enlarge as the fov location is removed further from the sub-satellite point.

* ECMWF Visiting Scientist on leave from Bureau of Meteorology Research Centre, Melbourne, Australia

In order to reduce the processing so that the output can be transmitted via the Global Telecommunication System (GTS) the HIRS and MSU data are processed in boxes. Presently these boxes are seven by nine arrays of HIRS scan spots and associated MSU data. The processing then computes the cloud free radiances in the boxes. This often has been referred to as the derivation of "clear-column" radiances. A complex objective analysis scheme is used to detect if there are truly clear scan spots within the array. If there are at least four, they are averaged to produced a radiance set for a "clear" sounding which is located at the centroid of the individual clear scan spots. If there are not a minimum of four clear spots, the array is processed to determine if there are enough partly cloudy areas which can pass a complex series of quality tests to be acceptable for further processing as a "partly cloudy" sounding. Finally, those arrays which fail these tests are classified as "cloudy". In the latter cases, the MSU channels and the four channels of HIRS which sense radiation from the highest part of the atmospheric column, those presumed not to be contaminated by cloud, are compiled for subsequent processing in the retrieval module as "cloudy" soundings. The use of a seven by nine array of HIRS fields of view gives a nominal horizontal resolution of the resulting soundings of about 250 km. (McMillin (1982)).

3. THEORY

3.1 Radiative Transfer Equation

The physical principal governing the temperature profile measurements is the same for all of these sensors. The temperature structure of the atmosphere is inferred from measurements of the earth's radiance in an absorption band due to a gaseous constituent whose concentration is uniform. (The 4.3μm CO_2, 15μm CO_2, and 5mm O_2 bands are used for the temperature profile sensing. Table 1 shows the TOVS sounding channels characteristics.) The instruments are designed to measure the radiance of different frequencies or wavelengths within one or more of these bands. By varying the frequency, one varies the level of the atmosphere from which the measured radiation originates. For example, absorption is most intense at the center of the band; consequently, this radiation emanates from only the very top of the atmosphere because of the strongest attenuation at lower levels. On the other hand, radiation arising from the lowest regions of the atmosphere can be measured at those frequencies far from the band center which are characterized by little absorption. Radiation received from intermediate levels is measured at frequencies associated with moderate absorption.

The outgoing radiance from earth measured by any channel of TOVS is related to the atmosphere's temperature and absorbing gas structure by the radiative transfer equation

$$R(\nu) = B_\nu[T(Po)]\,\tau_\nu(Po) - \int_o^{Po} B_\nu[T(p)]\,\frac{d\tau_\nu(p)}{dx(p)}\,dx(p), \qquad (1)$$

where $R(\nu)$ is the outgoing spectral radiance within a spectral channel centred at frequency ν, B_ν, the Planck radiance for temperature $T(p)$ at pressure p, $\tau_\nu(p)$ the transmittance of the atmosphere above pressure p, and $x(p)$ is an arbitrary function of pressure.

Table 1 TOVS sounding channels characteristics.

Channel Number	Channel Central Wavenumber	Central Wavelength (μm)	Principal Absorbing Constituents	Level of Peak Energy Contribution	Purpose of the Radiance Observation
1	668	15.0	CO_2	30 mb	Temperature Sounding. The 15 μm band channels provide better sensitivity to the temperature of relatively cold regions of the atmosphere than can be achieved with the 4.3 μm band channels. Radiances in Channels 5, 6, and 7 are also used to calculate the heights and amounts of cloud within the HIRS field of view.
2	679	14.7	CO_2	60 mb	
3	691	14.5	CO_2	100 mb	
4	704	14.2	CO_2	250 mb	
5	716	14.0	CO_2	500 mb	
6	732	13.7	CO_2/H_2O	750 mb	
7	748	13.4	CO_2/H_2O	900 mb	
8	898	11.1	Window	Surface	Surface Temperature and cloud detection.
9	1028	9.7	O_3	25 mb	Total Ozone concentration.
10	1217	8.3	H_2O	900 mb	Water Vapor Sounding. Provide water vapor corrections for CO_2 and window channels. The 6.7 μm channel is also used to detect thin cirrus cloud.
11	1364	7.3	H_2O	600 mb	
12	1484	6.7	H_2O	400 mb	
13	2190	4.57	N_2O	950 mb	Temperature Sounding. The 4.3 μm band channels provide better sensitivity to the temperature of relatively warm regions of the atmosphere than can be achieved with the 15 μm band channels. Also, the short-wavelength radiances are less sensitive to clouds than those for the 15 μm region.
14	2213	4.52	N_2O	850 mb	
15	2240	4.46	CO_2/N_2O	700 mb	
16	2276	4.40	CO_2/N_2O	600 mb	
17	2361	4.24	CO_2	5 mb	
18	2512	4.0	Window	Surface	Surface Temperature. Much less sensitive to clouds and H_2O than 11 μm window. Used with 11 μm channel to detect cloud contamination and derive surface temperature under partly cloudy sky conditions. Simultaneous 3.7 μm and 4.0 μm data enable reflected solar contribution to be eliminated from observations.
19	2671	3.7	Window	Surface	
20	14,367	0.70	Window	Cloud	Cloud Detection. Used during the day with 4.0 μm and 11 μm window channels to define clear fields of view.
MSU	Frequency (GHz)		Principal Absorbing Constituents	Level of Peak Energy Contribution	Purpose of the Radiance Observation
1	50.31		Window	Surface	Surface Emissivity and Cloud Attenuation determination.
2	53.73		O_2	850 mb	Temperature Sounding. The microwave channels probe through clouds and can be used to alleviate the influence of clouds on the 4.3 μm and 15 μm sounding channels.
3	54.96		O_2	500 mb	
4	57.95		O_2	100 mb	

In particular, the radiation received at frequency ν is the sum of all the radiance contributions from the earth's surface and from all individual levels in the atmosphere.

$$R(\nu_j) = \sum_{i=1}^{n} B[\nu_j, T(p_i)] w(\nu_j, p_i) \tag{2}$$

with

$$w(\nu_j, p_i) = \epsilon(\nu_j, p_i) \quad \tau(\nu_j, \sigma_{p_i})$$

In (2) $B[\nu_j, T(p_i)]$ is the Planck radiance source for the i^{th} pressure level (p_i), having a temperature T, ϵ (ν_j, p_i) is the emissivity of the emitting medium at the pressure p_j for radiation of frequency ν_j, τ (σ_{p_i}) is the transmissivity of the atmosphere above the i^{th} pressure level. $B(\nu, T)$ is explicitly

$$B(\nu, T) = C_1\nu^3/[\exp \quad (C_2\nu/T) - 1] \tag{3}$$

where C_1 and C_2 are the constants of the Planck function.

The term on the right of (2) is the sum of the component of radiance arising from the surface and all the radiation components originating in the atmosphere itself. These radiance contributions are weighted by the function $w(\nu_j, p_i)$. The weighting functions for TOVS instruments are illustrated in Fig. 1.

The problem is to determine the temperature of the N levels from radiance observations at say M discrete frequencies. However, because of the vertical width of the weighting functions, there is no unique solution; that is, many different temperature profiles will give rise to the same radiance measurements. Furthermore, the temperature profile solution tends to be unstable in the sense that small radiance measurement errors tend to produce disproportionately large errors of temperature.

The current operational retrieval method is based on regressions, however, eigenvector of both radiance and temperature are used in order to improve the regression noise level (Smith and Woolf, (1976)). A more detailed description of the theory is given in (Kelly, 1985).

4. ESTIMATION OF SPACIAL CORRELATION OF SATELLITE SOUNDING ERRORS

Currently the ECMWF Analysis System does not use satellite derived vertical temperature profiles over land in its Optimum Analysis, however, these profiles are processed by the assimilation system. The archived statistical data tapes contains these vertical profiles together with deviations from the six-hour forecast, analysis and initialization. This current study was conducted over the U.S. region since it provides a rich data area where the radiosonde network is of uniform type. There also have been other similar studies in this region. Hollingsworth and Lonnberg, and Lonnberg and Hollingsworth, in future referred HL (1984), also have computed the six-hour forecast error and also made estimates of the analysis error of the ECMWF assimilation system in this region.

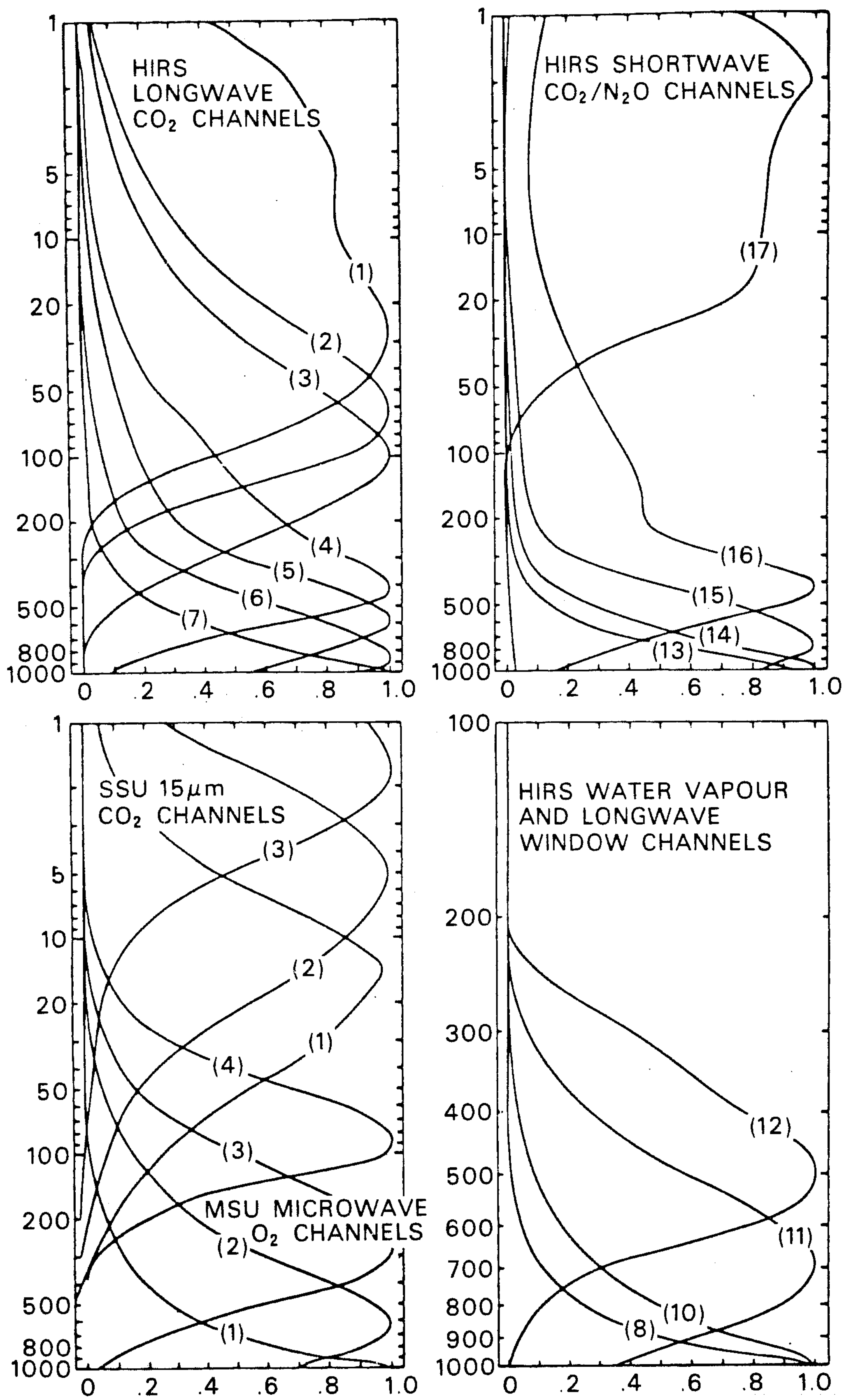

Fig. 1 TOVS normalized weighting functions.

Earlier work of Schlatter and Branstator (1979) have suggested that it is reasonable to neglect the observational interpolation error of the analysis grid over a dense data region, such as the Central United States. HL (1984) estimates of this error show it is much smaller than the error associated with satellite retrievals. It was also decided to use only 12Z radiosondes in this study to avoid any problems with radiosonde radiation corrections. Approximately 2000 satellite soundings (within ± 3 hours of these radiosondes) were used and this represented about one month of observations.

4.1 Horizontal Correlation

Next these data were sorted into bins of increasing distances of 100 km separations and the horizontal correlation was calculated for geopotential thickness layers of satellite observations minus analysis. Fig. 2(a) displays results of 300-200 mb thickness and Fig. 2(b) a comparison with earlier work of Schlatter (1980) using NMC Washington analyses and observations from TIROS-N. There is good general agreement in the structure however, the ECMWF length scale appears to be little shorter. The horizontal correlation of radiosonde observations minus ECMWF six-hour forecast was also calculated for comparison and is shown 2(c). These results are in good agreement with HL (1985) and provide a useful method of verifying the validity of all these calculations since it uses the same computation methods as the satellite correlations. The forecast correlation has a shorter length scale. The larger satellite scale is due to lack of vertical resolution in the tropopause region. This satellite length scale shortens at lower levels.

4.2 Vertical Correlation

The same data base that was used in the horizontal structure calculations was also used to calculate the vertical thickness error correlation from the ECMWF system. Fig. 3(a) shows the vertical correlation between all layer thicknesses between 1000 mb to 10 mb for the ECMWF analysis minus satellite observations. Fig. 3(b) compares results obtained from Schlatter (1980). Again there is good agreement. It is of interest to note the negative correlation that exists near the tropopause. This is again due to the lack of vertical resolution in the satellite soundings. Fig. 3(c) shows the vertical correlation of the ECMWF six-hour forecast minus radiosonde layer thicknesses. There is a quite different structure showing that the forecast error have little vertical correlation in contrast to their horizontal error structure.

5. DIRECT USE OF SATELLITE RADIANCE DATA

The HIRS instrument (from a single spacecraft) produces about one million sets of radiance measurements each day and it is not possible to use all these measurements in the ECMWF Global System. A number of limited area systems such as the PERIDOT (Durand 1985) make use these direct measurements, however, they only cover a limited geographical domains.

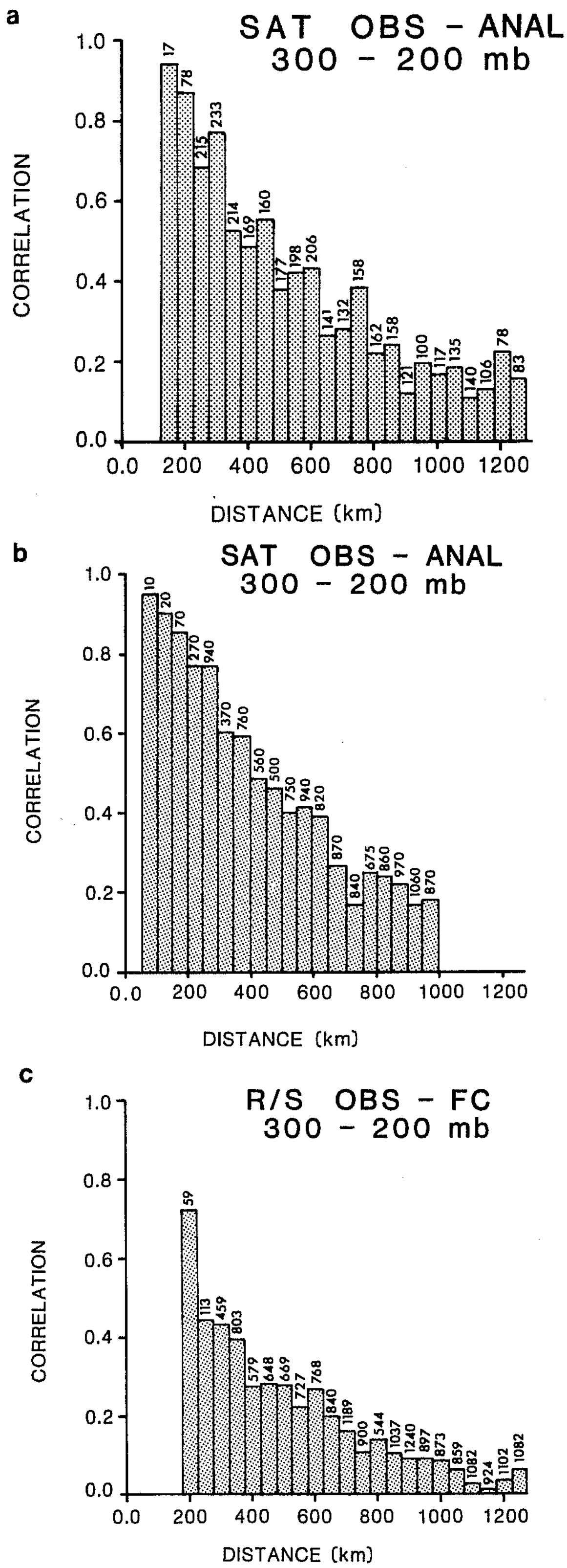

Fig. 2 (a) Horizontal Correlation for NOAA-7 NESDIS satellite retrievals minus ECMWF analysis in the North American region.

(b) Horizontal Corelation for TIROS-N NESDIS satellite retrievals minus NMC Washington analysis in the North American region.

(c) Horizontal Correlation for ECMWF six hour forecast minus US radiosondes.

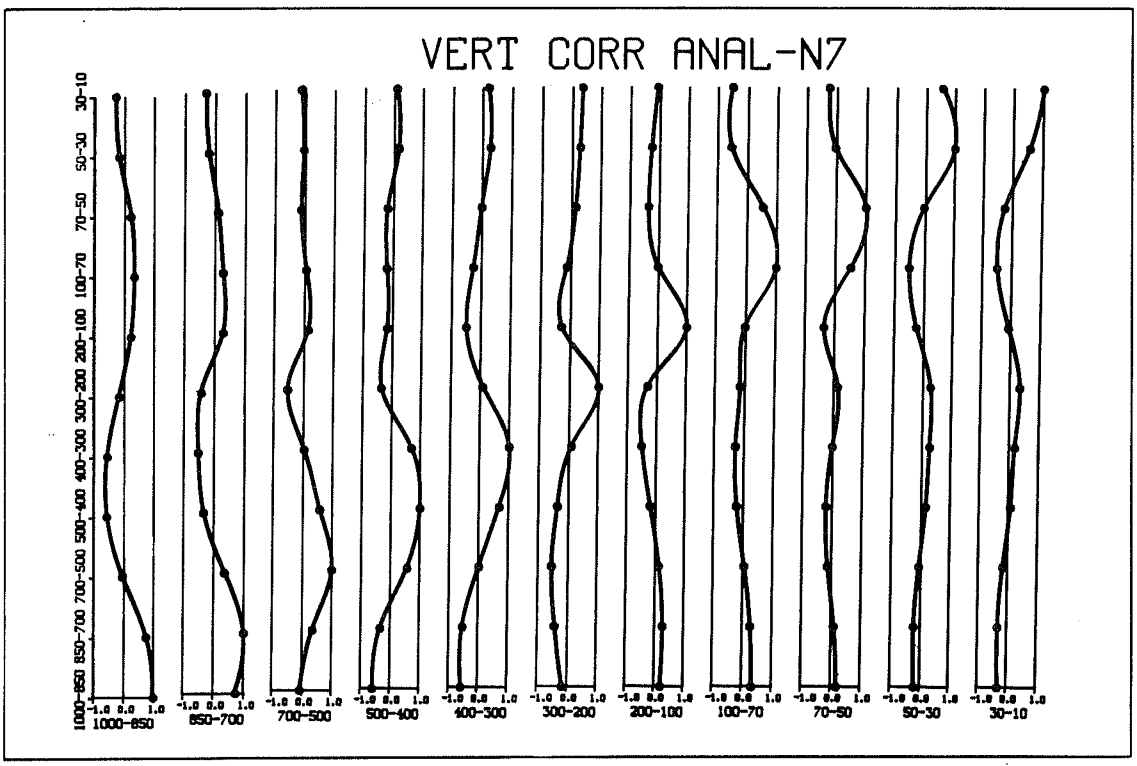

Fig. 3 (a) Vertical Correlation for ECMWF analysis minus NOAA-7, same data as Fig. 2(a).

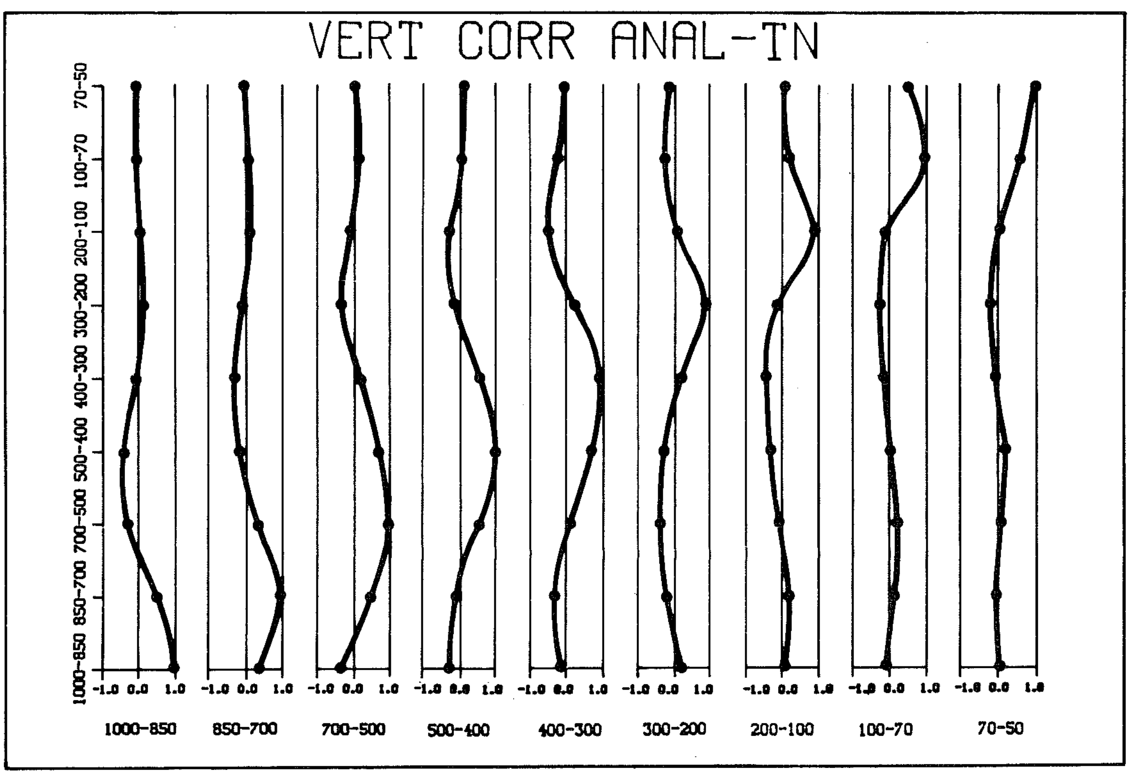

Fig. 3 (b) Vertical Correlation for NMC Washington analysis minus TIROS-N, same data as Fig. 2(b).

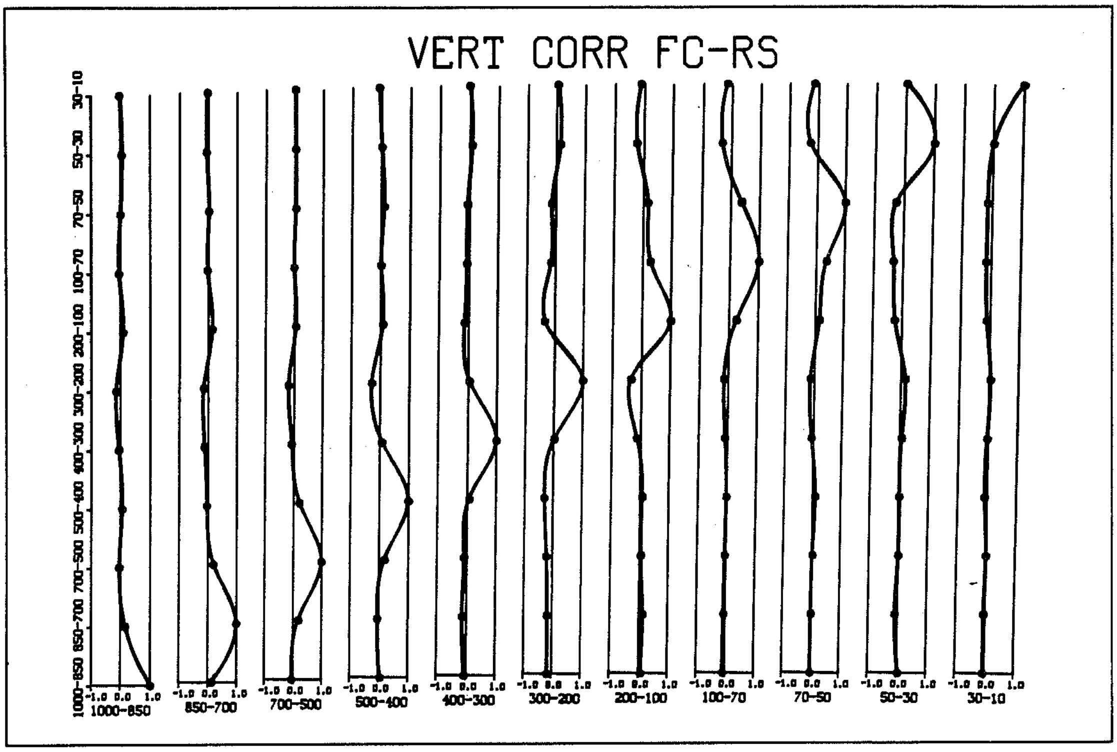

Fig. 3 (c) Vertical Correlation for ECMWF six hour forecast minus US radiosondes, same data as 2(c).

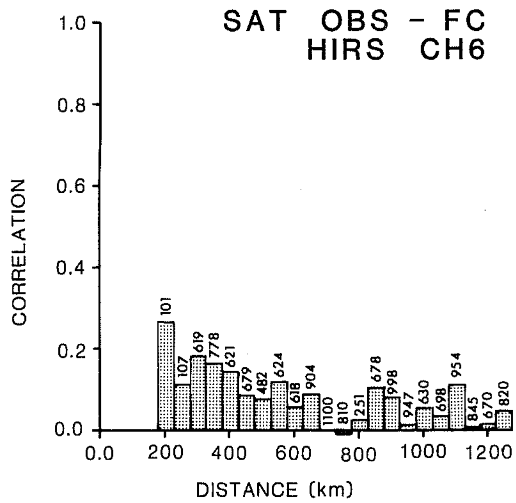

Fig. 4 (a) Horizontal Cross-Correlation of 850-700 mb geopotential thickness and HIRS channel 6 for ECMWF analysis minus US radiosondes.

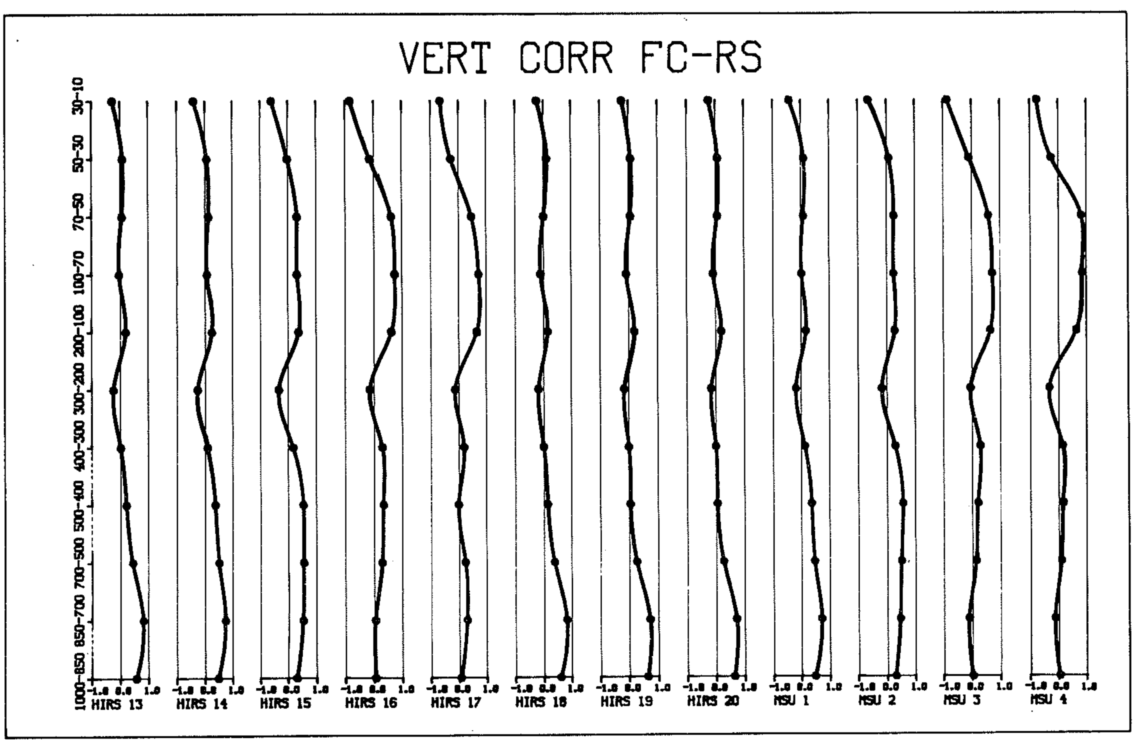

Fig. 5 (a) Vertical Cross-Correlation of all geopotential thickness layers and HIRS channels 13-20, MSU channels 1-4 for ECMWF analysis minus US radiosondes.

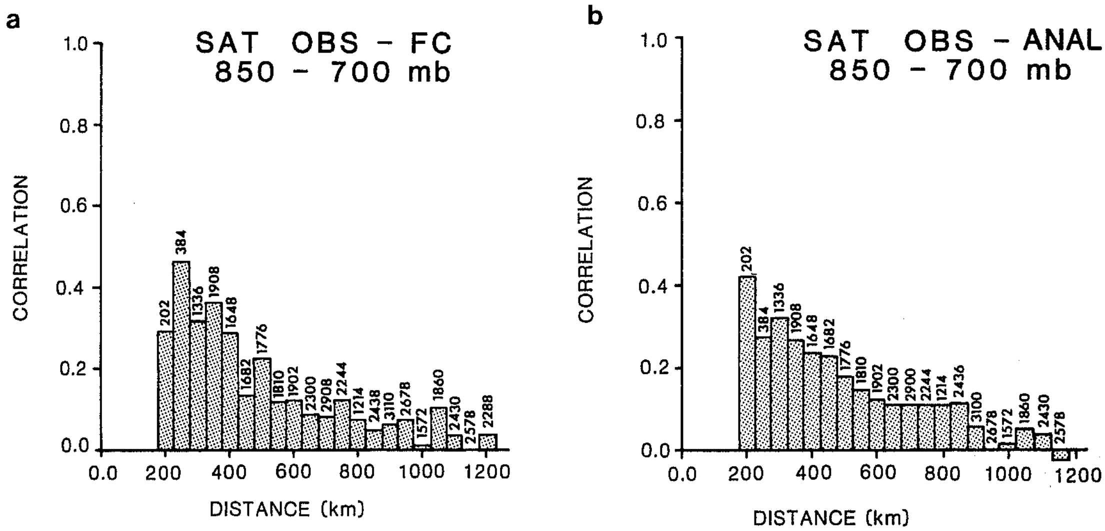

Fig. 6 (a) Horizontal Correlation of 850-700 mb thickness for ECMWF six-hour forecast using simulated radiance regression estimates minus simulated radiance regression estimates for radiosondes.

(b) As in 6(a) using ECMWF analysis in place of ECMWF six-hour forecast.

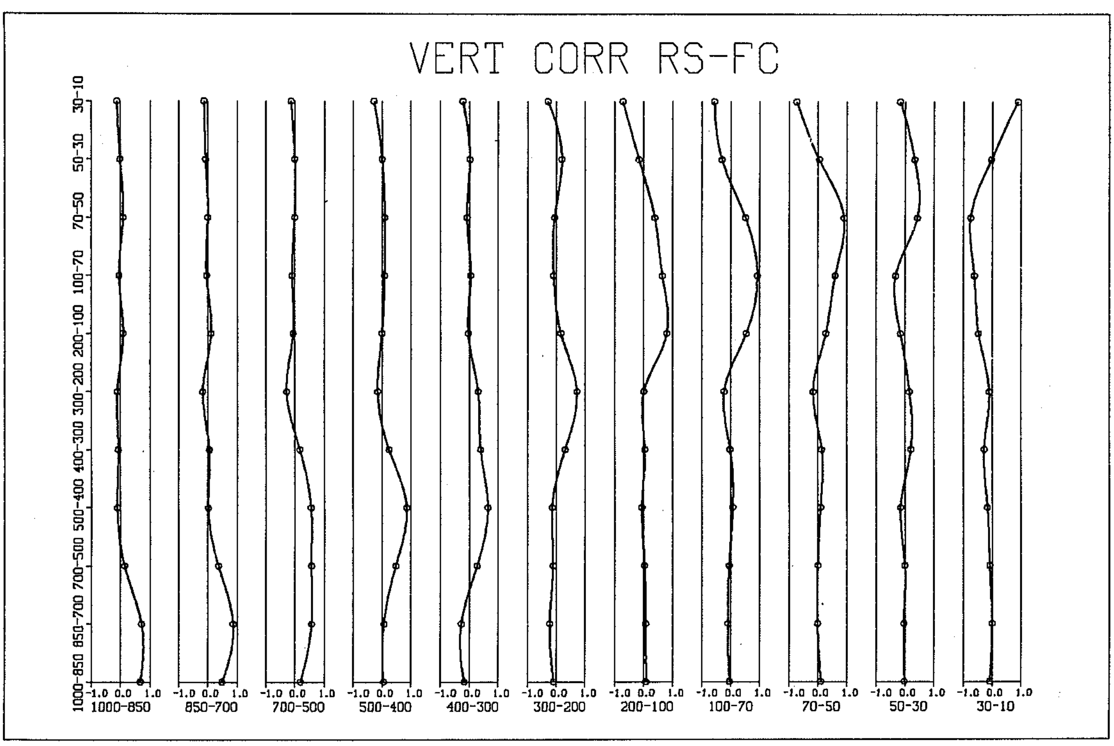

Fig. 7 Vertical Correlation for all ECMWF analysis levels of 6(a).

Many of these raw HIRS measurements are effected by cloud and this present study only uses the "clear-column" radiances as described in section 2. This reduces the number of satellite radiance sets of observation to about 2000 to 3000 per day for each satellite.

Currently the ECMWF statistics tape does not contain "clear-column" radiances which are required to calculate spacial radiance statistics. However, the U.S. radiosondes and the coincident six-hour forecast profiles used as input to a radiance simulation program. This forward calculation is now possible to within the accuracy of the HIRS instrument. Care had to be taken in this calculation to ensure the correct root mean squared noise value is used for each radiance channel. These noise estimates were obtained from NESDIS (Washington) by pairing "clear-column" radiances with simulated radiances produced from radiosonde flights.

The horizontal and vertical cross-correlations were then calculated between each analysis layer geopotential thickness differences and each HIRS and MSU radiance channel differences (i.e. radiosonde observations minus the ECMWF six-hour forecast cross-correlated with the computed radiance from radiosonde minus computed radiance from six-hour forecast). The same procedure as in Section 3 were used. Fig. 4 shows the results of the horizontal cross-correlation between 850-700 mb layer thickness error and HIRS channel 6 radiance error. This channel was chosen because its weighting function (Fig. 1) peaks about the 850-700 mb layer. It is disappointing that the cross-correlation of forecast error is so low. This is partly due to the high accuracy of the ECMWF six-hour forecast over the U.S. and also due to the noise in the clear-column radiances. Fig. 5 displays the vertical cross-correlations between channels 13-18 of HIRS and channel 1-4 of MSU. There is good agreement between these cross-correlations and the radiance weighting functions Fig. 1. However, it is clear that the signal to noise is a problem where cross-correlation is not strong. Another difficulty is the use of all 24 channels in the ECMWF Optimum Analysis would greatly increase the computational time.

In an attempt to overcome some of the above difficulties a linear regression was formed using all the forecast radiance errors (for each of 24 channels) as predictors to estimate the forecast geopotential thickness errors. This is similar to the statistical retrieval (Smith (1976)), however, there is an important difference, the regression does not impose the climatological mean profile on the solution. The regression only estimates the forecast deviation. Fig. 6(a) shows the forecast horizontal correlation for 850-700 mb geopotential layer. The results are much improved compared with the single channel radiance (Fig. 4) and are similar to the radiosonde correlation (Fig. 2(c)) but with a shorter length scale being a lower thickness layer. The computational overheads are also much less as only 14 thickness layers are input to the ECMWF Optimum Analysis.

The horizontal structure of the observational error of this simulated regression estimate was calculated (Fig. 6(b)) using the same method as section 4.1. This appears to have a much shorter length scale than the NESDIS satellite retrievals even considering that this result is at a lower level. It also is much shorter than Schlatter found for this thickness layer in this study (Schlatter (1980)).

Fig. 7 shows the vertical correlations of these simulated regression results for the six-hour forecast errors. Similar results for radiosonde layer thicknesses, as shown in Fig. 3(c), display much less inter-level correlation. This inter-level correlation in Fig. 7 is due to the width of the satellite weighting functions (Fig. 1) and suggests that the thickness layers should be increased. It appears that only five or six thickness layers should be estimated from the radiances.

6. CONCLUSIONS

The first part of this study gave good agreement with earlier work and provided some insight into the current performance of both the operational TOVS system, and the ECMWF assimilation system.

The second section highlighted some of the difficulties in using direct radiance measurements and the problems with signal/noise using a single radiance channel measurement, particularly in regions of high forecast accuracy. Multiple regression appears to improve this problem, however, the ECMWF analysis should be modified to accept thicker layers of geopotential thicknesses.

The next stage in this study is to fit the horizontal correlations with Bessel Functions similar to HL (1985) and to investigate other geographic regions. If the satellite clear-column radiances are added to the ECMWF statistic tape it will be possible to examine the geographic variation of forecast error.

The software will also be used to examine other satellite retrieval methods such as the physical method of Smith (1985). It is important when using these data to determine an extra term required in the Optimum Analysis which is the correlation between the first guess (forecast) and the satellite retrieval.

REFERENCES

Durand, Y. and R. Juvanon du Vachat, 1985: Developments of a Mesoscale Analysis using Raw Satellite Data. The Technical Proceedings of the Second International TOVS Study Conference Febuary 18-22.

Hollingsworth, A. and Lonnberg, P., 1985: The statistical structure of short range forecast errors as determined from radiosonde data. ECMWF data assimilation and observing system experiments with particular emphasis on FGGE 3-7 September 1984, 7-69.

Kelly, G.A., 1985: The Accuracy and Information Content of Satellite Atmospheric Vertical Profile Measurements. ECMWF Workshop on the Use and Quality Control of Meteorological Observations, 1984, 109-135.

Lonnberg, P. and A. Hollingsworth, 1985: The statistical structure of short-range forecast error as determined from radiosonde data. ECMWF data assimilation and observing system experiments with particular emphasis on FGGE 3-7 September 1984, 70-124.

McMillin, L.M. and Dean, C. 1982: Evaluation of a new operational technique for producing clear radiances. J. Appl. Met. 12, 1008-1014.

Schlatter, T.W. and Branstator, G.W., 1979: Estimation of errors in Nimbus 6 temperature profiles and their spatial correlation. Mon. Wea. Rev. 107, 1402-1413.

Schlatter, T.W. 1981: An assessment of operational TIROS-N temperature retrievals over the United States. Mon. Wea. Rev. 109, 110-110.

Smith, W.L. and Woolf, J.M., 1976: The use of eigenvectors of statistical covariance matricies for interpreting satellite sounding radiometer observations. J. Atmos. Sci., 33, 1127-1140.

Smith, W.L., Woolf, H.M., Hayden, C.M., Wark, D.Q. and McMillin, L.M., 1979: The TIROS-N Operational vertical sounder. Bull. Amer. Meteorol. Soc., 60, 1177-1187.

Smith, W.L. Woolf, H.M., Hayden, C.M. and Schreiner, A.J. 1985: The simultaneous retrieval export package. The Technical Proceedings of the Second International TOVS Study Conference Igls, February 18-22.